Smart Structures and Systems, *Vol. 27, No. 6 (2021) 1001-1010*
DOI: https://doi.org/10.12989/sss.2021.27.6.1001

Effect of agitation speed on microencapsulation of healing agent in PMMA shell and study on the mechanical properties of epoxy/PMMA microcapsules

Ramin Jahadi [1], Hamid Beheshti*[1], Mohammad Heidari-Rarani [1] and Amir H. Navarchian [2]

[1] *Department of Mechanical Engineering, Faculty of Engineering, University of Isfahan, Isfahan, 81746-73441, I.R. Iran*
[2] *Department of Chemical Engineering, Faculty of Engineering, University of Isfahan, Isfahan, 81746-73441, I.R. Iran*

(*Received August 15, 2020, Revised January 25, 2021, Accepted January 30, 2021*)

Abstract. In this study, the effect of agitation speed as a key process parameter on the morphology and particle size of epoxy-Poly (methyl methacrylate) (PMMA) microcapsules was investigated. Thus, a new interpretation is presented to relate between the microcapsule size to rotational speed so as to predict the particle size at different agitation speeds from the initial capsule size. The PMMA shell capsules containing EC 157 epoxy and hardener as healing materials were fabricated through the internal phase separation method. The process was performed at 600 and 1000 rpm mechanical mixing rates. Scanning electron microscopy (SEM) revealed the formation of spherical microcapsules with smooth surfaces. According to static light scattering (SLS) results, the average diameter size of the epoxy/PMMA capsules at two mixing rates were 7.49 and 5.11 μm for 600 and 1000 rpm, respectively, indicating that the mean size increased as the mixing rates of the process increased. The D_{50}, D_{90} and mean particle size values were the lowest for hardener/PMMA microcapsules at 1000 rpm. Moreover, the Fourier transform infrared (FTIR) spectroscopy was conducted to describe the chemical structure of epoxy and hardener PMMA capsules. To investigate the reinforcing role of microcapsules, they embedded in EPL-1012 epoxy resin with various amounts of 1 and 2.5 wt.% epoxy/PMMA capsules. The investigation also involved the effect of microcapsules on mechanical behavior as well as the reinforcement of polymer composite material. Experimental results showed that the tensile strength of the self-healing polymer composite slightly increased by 1 wt.% PMMA microcapsules prepared at 1000 rpm and then reduced with an increase in the concentration and mean size diameter of PMMA microcapsules. In addition, a similar trend of Young's modulus was seen for pristine epoxy matrix and microcapsule-loaded epoxy composite.

Keywords: self-healing; PMMA microencapsulation; epoxy composite; reinforcing properties

1. Introduction

Due to their exceptional specific mechanical properties compared to conventional materials, polymer matrix composites have become highly utilized in great industries like aerospace, energy, automotive and offshore structures (Drenchev and Sobczak 2014, Andersson *et al*. 2007). In spite of using polymers as a higher performance matrix in composites, damages including matrix cracking and microcracking can be of significant detriment to performance during their action in structural applications (Bolimowski *et al*. 2016, Omosola *et al*. 2015). Microcracks occur very often within a structure and then propagate through the material and ultimately leading to premature failure. Self-healing materials have attracted great attention in polymer composites where they can repair microcracks independently. This repair takes place with no detection techniques or a particular manual intervention through a range of approaches (Hillewaere and Du Prez 2015, Wang *et al*. 2015, Urdl *et al*. 2017, Zhai *et al*. 2020), including embedding microcapsules (Zhu *et al*. 2015, Sharma *et al*. 2018, Taheri *et al*. 2020, Sun *et al*. 2019), hollow fibers (Kousourakis and Mouritz 2010, Trask and Bond 2006) and microvascular networks (Luterbacher *et al*. 2016, Omosola *et al*. 2014) filled with healing agents. It is expected that durability, safety, and reliability of materials will improve through self-healing, while the cost associated with repair and maintenance will decrease, leading to long-lived materials (Wang *et al*. 2015, Souzandeh and Netravali 2019). In the encapsulation-based healing system, dispersed microcapsules are ruptured by a propagating crack to release the healing agent and react with the crack surface to heal the damaged region (Blaiszik *et al*. 2010).

Being widely acknowledged as one of the most popular techniques, encapsulation of healing agents is classified in various types, including single capsules and double-capsules, depending on the encapsulation of healing agents and curing agents in the same or separate capsules, respectively. Several studies have been conducted to utilize the double-capsule system. Ahangaran *et al*. (2016, 2017a, b) investigated microencapsulation of low viscosity epoxy resin healing agent along with mercaptan curing agent in PMMA wall material and prepared self-healing epoxy composite. Yuan *et al*. (2008, 2009) developed epoxy/mercaptan microcapsules as a two-component healing agent utilizing poly (melamine-formaldehyde) (PMF) shell. They embedded the capsules in the epoxy matrix and evaluated the repair effectiveness of agents. The self-healing

*Corresponding author, Ph.D., Associate Professor,
E-mail: hamid.beheshti@eng.ui.ac.ir

ISSN: 1738-1584 (Print), 1738-1991 (Online)

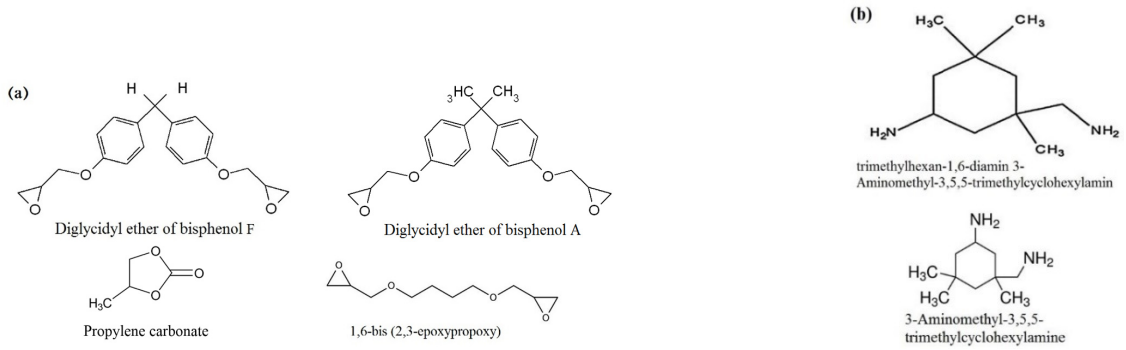

Fig. 1 Molecular structure of components in epoxy mixture (a) and the main component of hardener (b)

performance of the polymer composite using diglycidyl ether of bisphenol A type epoxy and polyether-amine hardener as the core materials with PMMA shell material is reported by Li *et al*. (2013a).

The main process parameters of microencapsulation using the solvent evaporation technique are; viscosity of healing agents, polymer molecular weight, core/shell ratio, polymer concentration, dispersion rate, mechanical mixing speed, etc. (Zhu *et al*. 2015, Ahangaran *et al*. 2017b, Li *et al*. 2013a). Recent research on certain factors is reviewed herein. Due to the strong shear force under a high mixing rate, the mean diameter of microcapsules diminishes with an increase in agitation speed (Li *et al*. 2013a). Moreover, the higher core/shell ratio results in the formation of imperfect capsules during the microencapsulation process. The polymer molecular weight of shell material affects the surface morphology of microcapsules. In fact, the high molecular weight can develop spherical and almost monodisperse micelles with high aggregation (Ahangaran *et al*. 2016). As an indicator of the effect of these factors, the mechanical behavior of the microcapsules containing the healing agent through the matrix polymer is evaluated (Hu *et al*. 2020, Kosarli *et al*. 2019, He *et al*. 2019).

The self-healing performance and mechanical behavior of epoxy composites have been studied from various aspects. Wang *et al*. (Wang *et al*. 2010, Li *et al*. 2008) found the influence of interfacial adhesion and surface morphology between the epoxy matrix and microcapsule shell on improving tensile and impact resistance strength of self-healing composite. Lee *et al*. (2012) studied the micromechanical behavior of epoxy and mercaptan containing microcapsules in poly(melamine-formaldehyde) (PMF) shell through nanoindentation. The healing efficiency of dual-components PMMA microcapsules with various amounts of capsules was investigated on the tapered double cantilever beam (TDCB) specimens by Li *et al*. (2013b) who achieved 84.5% healing efficiency with 15 wt.% microcapsules. Kim *et al*. (2019) reported the self-healing of fatigue damage in unidirectional glass/epoxy laminated composites with embedded microcapsules. Ahangaran *et al*. (2019) evaluated the tensile strength and elastic modulus of the microcapsule-loaded epoxy composite.

The present study examines the effect of a two-component healing agent system, including low viscosity epoxy as the polymerizable healing agent and hardener as the curing agent on EPL-1012 matrix polymer. Despite investigating different chemical and physical parameters in previous studies on PMMA microcapsules (Ahangaran *et al*. 2016), a new relationship was proposed to predict capsule size at different rotational speeds in this study. Therefore, epoxy/hardener in a PMMA shell with higher molecular weight was encapsulated by the solvent evaporation method first, and then microcapsules formation was characterized. The mechanical behavior of epoxy composite via microencapsulated EC 157 epoxy resin and W 152 MLR hardener in PMMA shell has not been studied in the literature. Thus, the reinforcing role of microcapsules with different capsule sizes and various amounts of the intended microcapsules through the matrix polymer was evaluated.

2. Materials and experiments

2.1 Materials

EPL-1012 bisphenol F type epoxy resin and EPH-112 (amine base) hardener with the weight ratio of 100/12 were used as the matrix polymer. As a healing agent for microencapsulation, low viscosity EC 157 epoxy polymer and corresponding hardener containing a mixture of amines (W 152 MLR) obtained from Elantas Co., Italy were used. The EC 157 composition was 30–50% bisphenol F diglycidyl ether (DGEBF), 30–50% bisphenol A diglycidyl ether (DGEBA), 20–30% 1,6-bis (2,3-epoxypropoxy) hexane and < 5% propylene carbonate. The molecular structure of components in epoxy mixture and hardener are indicated in Fig. 1. The viscosity of epoxy, hardener, and the healing agents are listed in Table 1. PMMA, with the molecular weight of 140,000 g/mol, was purchased from LG Co., Korea as the capsule wall material. Dichloromethane (DCM) and sodium dodecyl sulfate (SDS) were obtained as a solvent and as an emulsifier from Merck Co., Germany, respectively. The materials were used as received.

2.2 Microcapsule and epoxy-based composite preparation

Due to the ease of capsule fabrication of hydrophobic materials and obtaining better surface morphology, the

Table 1 The viscosity of epoxy, hardener and healing agents (factory datasheet)

Material	Viscosity at 25°C (mPa.s)
EPL 1012	900-1100
EPH 112	30
EC 157	500-600
W 152 MLR	5-20

phase separation technique was conducted for encapsulation of epoxy (EC 157) and hardener (W 152 MLR) as the core materials and PMMA as the capsule wall (Bekas *et al*. 2016). The one-to-one ratio of EC 157 (0.5 g) and PMMA (0.5 g) were poured separately into 30 ml DCM. Afterwards, the mixed oil phase was distributed dropwise into 50 ml of 1 wt.% aqueous SDS solution under 600 and 1000 rpm mixing rates for one hour at ambient temperature to achieve an oil/water emulsion. Thereafter, the resultant emulsion became poured into 100 ml of 1 wt.% emulsifier solution under continuous auto-mechanical mixing. Finally, the emulsion was stirred in a magnetic stirrer at ambient temperature to evaporate dichloromethane and obtain PMMA capsules. The microcapsules became filtered, washed several times with deionized water and then dried at ambient temperature. Similarly, the above process was used for the preparation of the hardener/PMMA capsule. Finally, the yield of microencapsulation was measured according to the following formulation by determining and specifying the ratio of the gathered capsules weight, w, to the total weight of the core material contents (w_{core}) and PMMA shell contents (w_{shell}) (Navarchian *et al*. 2019)

$$\alpha = \left[\frac{w}{w_{core} + w_{shell}}\right] \times 100\% \quad (1)$$

2.3 Characterization

The chemical structures of PMMA as wall material, EC 157 and W 152 MLR as core materials were characterized using FTIR spectroscopy. The measurements were performed with Jasco equipment (6300 model) in the wavenumber span of 500-4000 cm^{-1} with a resolution of 4 cm^{-1}. The core content of the prepared microcapsules was determined using thermogravimetric analysis (TGA) instrument (Rheometric Scientific STA 1500, USA) under nitrogen atmosphere and with heating rate of 10°C min^{-1}. The morphology examination of capsules was conducted by optical microscopy (Olympus, Japan) and scanning electron microscopy (SEM, VEGA\\TESCAN, Czech Republic) at 15.0 kV. The particle size distribution of oil/water emulsion of healing agent microcapsules was measured using static light scattering (SLS, Malvern Instruments Ltd, UK). The instrument was able to detect droplets ranging from 0.02 μm to 1000 μm.

2.4 Mechanical testing of self-healing epoxy composite

In order to investigate the reinforcing role of microcapsules and interface bonding of capsule shell and matrix, PMMA microcapsules containing EC 157 and W 152 MLR with a constant weight ratio of 1:1 were embedded in EPL-1012 epoxy resin and EPH-112 hardener as a matrix polymer. After degassing, the pristine epoxy and self-healing epoxy composite containing 1 and 2.5 wt.% of PMMA microcapsules were poured into the mold. The dumbbell shape specimens with a 50 mm gauge length were prepared following the ASTM D638 (2014), type I specimen standard. The samples were cured for one day at ambient temperature and post-cured at 90 °C for two hours. The tensile tests were conducted with a speed of 1 mm/min at ambient temperature with a servo-controlled tensile machine. An extensometer was attached to the gauge section of all specimens and the tests were performed in a strain-controlled mode. The general view of tensile specimen mold and test setup are shown in Fig. 2.

3. Results and discussion

In this section, the chemical structure of PMMA microcapsules and successful microencapsulation are evaluated first and then the morphology and particle size distribution of microcapsule are explained. Finally, the mechanical behavior of the microcapsules through the matrix polymer is discussed.

Fig. 2 The general view of tensile specimen mold (a) and test setup (b)

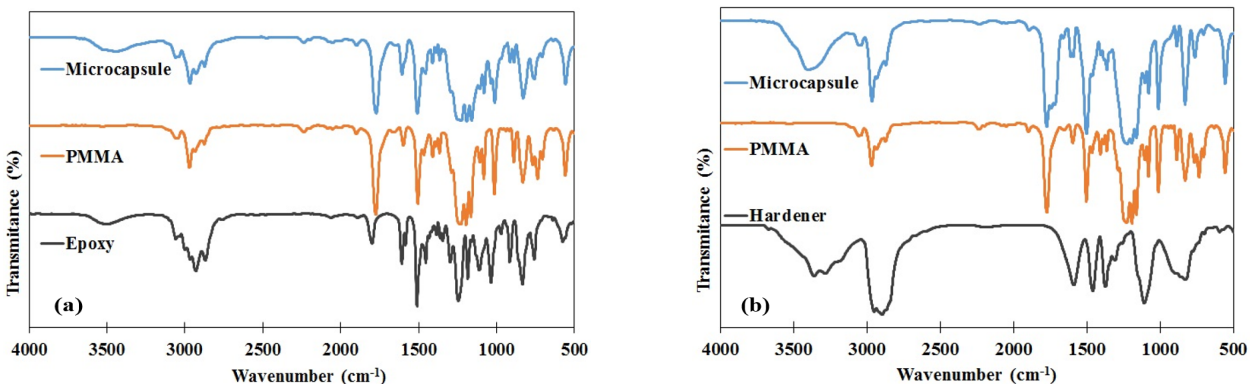

Fig. 3 FTIR spectra of (a) EC 157, PMMA and epoxy microcapsules; and (b) W 152 MLR, PMMA and hardener microcapsules

3.1 Characteristics of epoxy and hardener PMMA microcapsules

The FTIR spectra of PMMA, epoxy and epoxy/PMMA microcapsules are depicted in Fig. 3(a). The FTIR spectrum of EC 157 reveals a stretching absorption peak of C-O-C at 832 cm^{-1}. Moreover, the absorption peaks at 915, 1243 cm^{-1} and also the C-O deformation band stretching vibration of the oxirane group are related to one another, in a respective manner (Ahangaran *et al*. 2019). The absorption peaks at 2869 and 2997 cm^{-1} are assigned to the stretching vibrations of the C-H band in aliphatic and aromatic rings of the epoxy chemical structure, respectively. The broad absorption peaks at 3500 cm^{-1} denote the -OH stretching vibration (Theophile 2012).

An absorption peak at 1160 cm^{-1} is demonstrated by the FTIR spectrum of the PMMA shell material, i.e., it relates to the C-H band of -$COOCH_3$ group (Duan *et al*. 2008). The distinctive peak at a wavenumber of 1199 cm^{-1} and stretching peak at 1231 cm^{-1} are related to the O-CH_3 band and C-O-C group, respectively. Furthermore, owing to the presence of the C=O group, the stretching peak appears at 1774 cm^{-1}. There are symmetric and asymmetric stretching vibrations of the C-H band in the neat PMMA shown at 2874 and 2969 cm^{-1}, respectively (Suryanarayana *et al*. 2008). The entire characteristic peaks of both epoxy and PMMA appearing on the FTIR spectrum of EC 157/PMMA microcapsules confirm successful encapsulation.

In Fig. 3(b), the FTIR spectrum of hardener shows the plane bending of N-H at 830 cm^{-1}, bending modes of CH_2 at

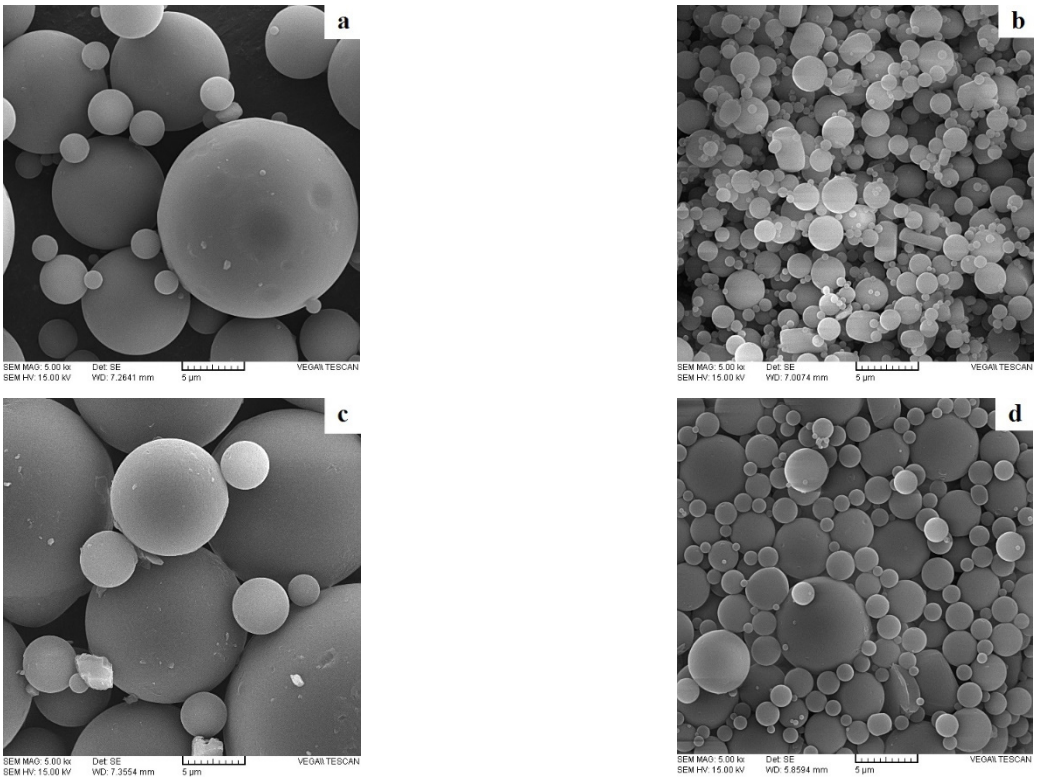

Fig. 4 SEM micrographs of the epoxy- and hardener-contained microcapsules for the mechanical mixing rate of (a)-(b) 1000 rpm and (c)-(d) 600 rpm, respectively

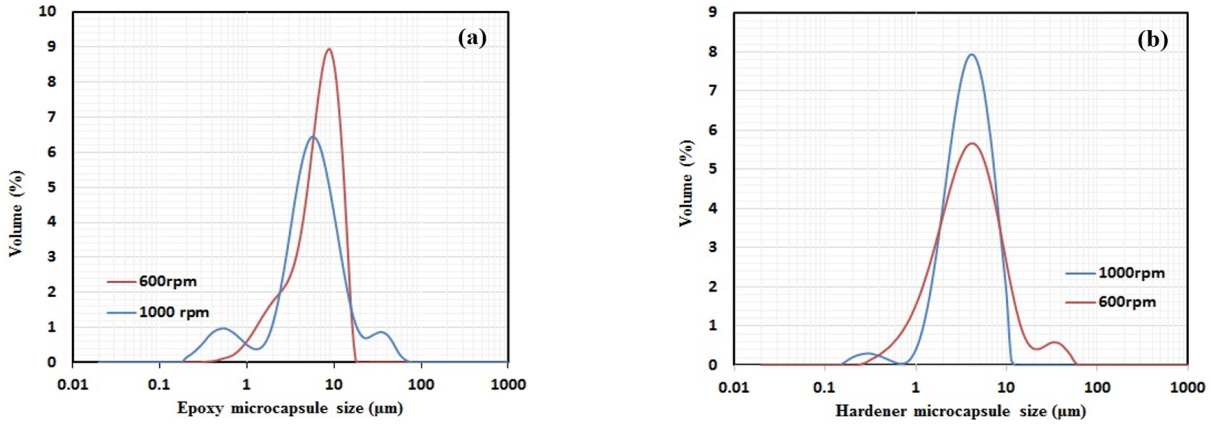

Fig. 5 Particle size distribution measured by SLS of the (a) epoxy and (b) hardener with PMMA shell for 1000 and 600 rpm mechanical mixing rate

1460 cm^{-1}, and broad absorption peak of N-H band at 1590 cm^{-1} (Li *et al*. 2013a). The stretching vibration peaks at 2899 and 2953 cm^{-1} represent the C-H band in the hardener structure. The peaks at 3287 and 3362 cm^{-1} are due to the O-H and N-H stretching bonds 3362 cm^{-1} are due to the O-H and N-H stretching bonds, respectively. The spectrum of the hardener/PMMA capsules underwent all the characteristic peaks of hardener and PMMA. This indicates the possible formation of hardener microcapsules, though further evidence is necessary to show the exact morphology.

3.2 Morphology of prepared PMMA microcapsules and size distribution

The SEM micrographs of the EC 157/PMMA and W 152 MLR /PMMA microcapsules at two different mechanical mixing rates of 1000 and 600 rpm are illustrated in Fig. 4. Under all conditions, the spherical shape and smooth surface morphology of capsules with similar morphology to those reported in the literature are formed (Sharma *et al*. 2018, Navarchian *et al*. 2019, Ullah *et al*. 2016). Regarding the geometrical form of the microcapsules, the majority of encapsulation techniques provide the synthesis of spherical microcapsules (Zhu *et al*. 2015).

Fig. 5 shows particle size distribution using static light scattering (SLS) of (a) epoxy and (b) hardener PMMA microcapsules for 1000 and 600 rpm mechanical mixing rate. The epoxy/PMMA emulsion at 1000 rpm exhibited the broader size distribution in comparison to the similar emulsion at 600 rpm (Figs. 4(a), (c)). The emulsion containing hardener/PMMA microcapsules at 1000 rpm showed narrower particle size distribution than hardener/ PMMA emulsions at 600 rpm (Fig. 4(b), (d)). Moreover, the peak height was more significant compared to the emulsion at 600 rpm.

In order to determine the average shell thickness of the PMMA microcapsules, a rational method between the volume fractions of core/shell material, mean core content, and mean diameter of microcapsules was employed. The total volume of capsule includes the volume of shell and core content i.e.

$$V_{total} = V_{shell} + V_{core} \tag{2}$$

which can be written as

$$V_{total} = V_{shell} + v_C V_{total} \tag{3}$$

where v_c is volume fraction (vol%.) of core content. For a two-component substance with different density values, the following relation is used to calculate volume fraction from weight fraction

$$v_c = \frac{1}{1 + \frac{\rho_c}{\rho_s}\left(\frac{1}{w_c} - 1\right)} \times 100 \tag{4}$$

where ρ_c, ρ_s and w_c are core density (EC 157:1.15 g/cm^3 and W 152 ML:0.95 g/cm^3), shell density (1.18 g/cm^3) and core content weight fraction, respectively. The weight fraction of core content is obtained from TGA analysis. According to the spherical shape of microcapsules ($V = \frac{4}{3}\pi R^3$), and performing a few simple mathematical operations on Eq. (3), the following equation can be determined

$$R_{int} = \sqrt[3]{v_c R_{ext}^3} \tag{5}$$

where R_{int} and R_{ext} are the mean internal and external capsule radius, respectively. Therefore, the average shell thickness of microcapsules is obtained by difference of internal and external radiuses.

The mean size values of D_{10}, D_{50}, and D_{90}, core content, shell thickness, and yield of microencapsulation at different circumstances are presented in Table 2. It should be noted that the D_x diameter is the particle diameter amounting to x% cumulative undersize particle size distribution. The yield of microencapsulated healing agents was obtained in the range of 72-78% and 67-70% for epoxy and hardener microcapsules, respectively. The results show that the yield of healing agent capsules increased as the mechanical mixing rate decreased. The increase in yield could be

Table 2 The measured parameters of epoxy/PMMA and hardener/PMMA microcapsules

Sample	Mixing rates (rpm)	Yield (%)	D_{10} (μm)	D_{50} (μm)	D_{90} (μm)	Mean size (μm)	Core content (wt.%)	Shell thickness (μm)
EC 157/PMMA	1000	72	1.48	5.01	9.15	5.11	62	0.73
EC 157/PMMA	600	78	2.25	7.35	12.76	7.49	51	1.48
hardener/PMMA	1000	67	1.83	4.03	7.76	4.09	80	0.24
hardener/PMMA	600	70	1.30	4.06	10.24	5.67	68	0.57

related to the increasing mean particle size of the emulsion prepared by SDS as an emulsifier, leading to more efficient separation and collection of resultant capsules (Ahangaran *et al*. 2016). The D_{50}, D_{90} and average particle size values were the lowest for hardener/PMMA microcapsules at 1000 rpm. From D_{50} and D_{90} values, it can be deduced that emulsion made with epoxy/PMMA microcapsules at 600 rpm had 50% of droplets below 7.35 μm and 90% of droplets below 12.76 μm, which were the largest table values. The average diameter size of the epoxy/PMMA microcapsules were 7.49 and 5.11 μm for 600 and 1000 rpm, respectively, indicating lower mixing rate and higher mean size values of microcapsules. In a similar trend, the average particle sizes for the hardener/PMMA microcapsules were 5.67 and 4.09 μm for 600 and 1000 rpm, respectively. Navarchian *et al*. (2019) prepared single PMMA microencapsulated linseed oil at three different mixing speeds of 1000, 600 and 300 rpm. The mean particle size of the capsules was in the range of 2.6, 5.45 and 11.65μm for 1000, 600, and 300 rpm, respectively. Further, Li *et al*. (2013a) reported that the average diameter size of microcapsules diminishes with a rise in the mixing rate. In fact, an increased mechanical mixing speed caused the shear forces to overcome the interfacial tension forces as well as the very fine droplets from the capsules (Ullah *et al*. 2016, Tong *et al*. 2010). The various elements, including the hydrodynamic condition and the physical chemistry of core/shell material, could be affected in the produced capsules size (Sun *et al*. 2020, Yan *et al*. 2019).

In order to evaluate agitation speed as a key process parameter on the particle size of microcapsules, an analogy between a system of rotational rheometer and propeller blades of mechanical mixing was made. Shear rates for rotational rheometer were defined as in the following equations (Schramm 1994)

$$\dot{\gamma} = \frac{1}{tan\,\alpha} \cdot \Omega(s^{-1}) \tag{6}$$

where α is the cone angle of rheometer, which can be equivalent to the propeller blade angle and Ω is the angular velocity of the rotor that is corresponding to the angular velocity of blades, as determined

$$\Omega = \frac{2\pi \cdot n}{60} \left(\frac{rad}{s}\right) \tag{7}$$

where n is the rotor speed that is equal to the agitation speed. The comparison between two mechanical mixing rates leads to the following relation

$$\frac{\dot{\gamma}_{1000rpm}}{\dot{\gamma}_{600rpm}} = \frac{n_{1000rpm}}{n_{600rpm}} \tag{8}$$

According to the experimental results, the mean size diameter of microcapsules (D) has an antagonistic relationship with agitation speed. Therefore, it can be defined

$$\frac{D_{1000rpm}}{D_{600rpm}} = f(\eta, M_v, R, T, t, \dots)\frac{\dot{\gamma}_{600rpm}}{\dot{\gamma}_{1000rpm}} = f(\eta, M_v, R, T, t, \dots)\frac{n_{600rpm}}{n_{1000rpm}} \tag{9}$$

In this equation, f is considered as a function depending on various factors such as material properties of core/shell polymer containing viscosity (η), molecular weight (M_v), etc and processing parameters such as core/shell ratio (R), Temperature (T), time (t), and also uncertainties.

Due to the identical material properties and assuming the exact processing parameters during capsule preparation (epoxy or hardener), all factors became equal and the above equation can be written as

$$\frac{D_{1000\,rpm}}{D_{600\,rpm}} \simeq \frac{n_{600\,rpm}}{n_{1000\,rpm}} \tag{10}$$

which this can be simplified

$$D_2 \simeq \frac{D_1 n_1}{n_2} = D_1 n_1 x^{-1} \tag{11}$$

Fig. 6 depicts the effect of the rotational speed on the mean size diameter of three types of microcapsules. In this figure, the experimental values were plotted versus the predicted values, which obtained from the above relationship (11). The average diameter size of PMMA/Lo, composite microcapsules (CM), and Urea-Formaldehyde (UF)/epoxy microcapsules were reported in the range of 2.6-11.65, 35-154 and 64–411 μm, respectively (Kosarli *et al*. 2019, Navarchian *et al*. 2019, Sun *et al*. 2020). The comparison of the experimental values and analogy relation values (Eq. (11)) indicated the same trend of reduction in capsule size as the mixing rate increased.

The difference between the data can be attributed to the unintended changes in the encapsulation process conditions and uncertainties. For obtaining a more precise relationship, the curve-fitting is done on the experimental values using the curve-fitting tool of MATLAB software and the best one

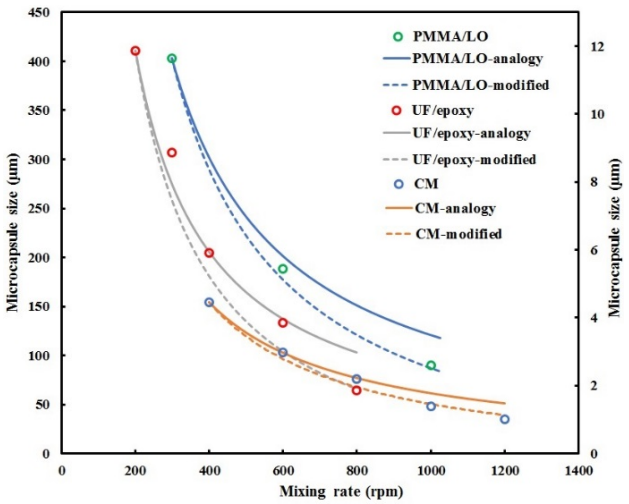

Fig. 6 Comparison of mean size diameter of the experimental values and predicted values of analogy relation and modified analogy relation

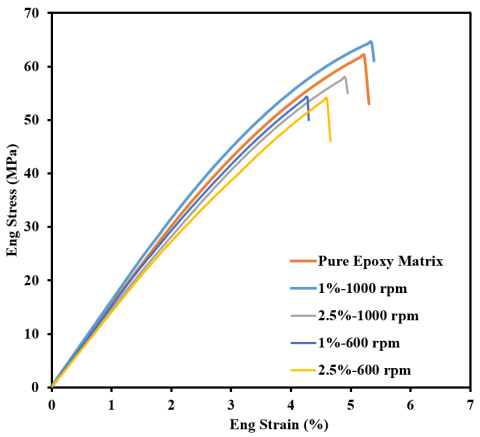

Fig. 7 Engineering tensile stress-strain curves of pure epoxy and epoxy composites samples containing various microcapsule content

is selected with R^2 above 0.98 through the following equation

$$y = ax^{-1} + b \tag{12}$$

Therefore, the modified relationship is recommended as follows

$$y = \beta D_1 n_1 x^{-1} + b \tag{13}$$

where β is a correction coefficient, suggested as 1.12 and b is the offset between the value obtained from the equation and the experimental value at the initial point

$$b = D_1(1 - \beta) = -0.12D_1 \tag{14}$$

The modified curves are also shown in Fig. 6. Therefore, the particle size in different agitation speeds could be predicted from the initial microcapsule size using the two aforementioned equations. Accordingly, based on the mean size diameter of the epoxy and hardener microcapsules for 600 rpm, it is expected to achieve 4.5 and 3.5 μm for 1000 rpm. However, there is an almost 13% difference between the actual data and the analogy relationship values. To further investigate the analogy relationship, more data at different mixing rates are needed.

3.3 The reinforcing role of healing microcapsules

To evaluate the effect of microencapsulated dual-component healing agents on the mechanical behavior of self-healing composites, the tensile tests were performed on the specimens filled with dual-component microcapsules. Besides, the influence of capsule size produced by 1000 and 600 rpm mixing rate and various amounts of 1 and 2.5 wt.% of EC 157- and W 152 MLR-loaded PMMA microcapsules were investigated. According to the earlier research (Ahangaran *et al*. 2019), the tensile strength (TS) of pristine epoxy decreased with increasing the incorporation of PMMA capsules ranging from 2.5 to 10 wt.%. That is why the lower amounts of microcapsules are selected in this study. Fig. 7 illustrates the tensile engineering stress-strain test plots of pristine epoxy matrix and self-healing epoxy

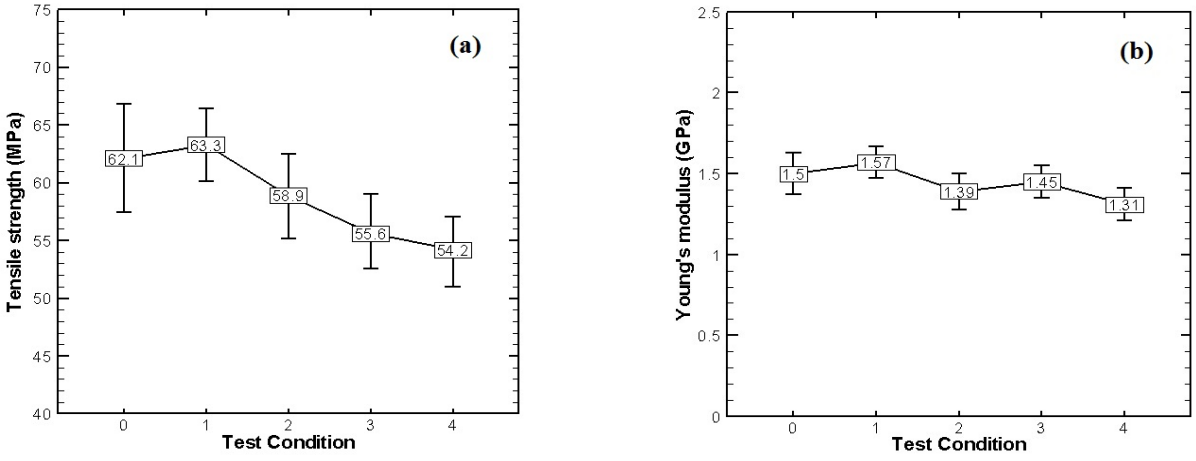

Fig. 8 (a) Tensile strengths and (b) Young's modulus of the epoxy-based self-healing composites at different test conditions of pure epoxy (0), 1 and 2.5 wt.% of microcapsule content at 1000 rpm (1,2) and 1 and 2.5 wt.% of microcapsule content at 600 rpm (3,4)

composite at room temperature. The tensile strength of the dual-component PMMA microcapsules embedded epoxy matrix with 1 wt.% of PMMA microcapsules content at 1000 rpm shows a limited increase in comparison to the virgin epoxy matrix. On the contrary, the TS is dropped in the specimens with 2.5 wt.% of microcapsules. At 600 rpm mixing rate, the tensile strength of both 1 and 2.5 wt.% self-healing microcapsule-loaded epoxy system decreased as compared with the pure epoxy matrix by about 5 and 8 MPa, respectively (Fig. 8(a)). This could be related to the increase in the mean size diameter of microcapsules. The weak connection between the epoxy matrix and the microcapsule wall on the one hand, and behavior and function of microcapsules as a defect at the cross-section of the matrix on the other hand are considered as the two main factors effective in the reduction of TS in self-healing epoxy composites (Zhang *et al*. 2014). The mechanical properties of epoxy composites with incorporated PMF capsules which contained epoxy and mercaptan healing agents were evaluated by Yuan *et al*. (2008). They found a continued trend of decrease in the tensile strength. The initial rise in tensile strength of self-healing epoxy composite specimens in comparison with virgin epoxy can be attributable to the enhanced toughness brought about by embedding the thermoplastic PMMA wall (Li *et al*. 2013b).

Fig. 8 depicts the trends of Young's modulus and tensile strengths concerning different test specimens containing pure epoxy and various amounts of 1 and 2.5 wt.% PMMA microcapsules at the agitation speed of 1000 and 600 rpm. Fig. 7(b) shows that Young's modulus of 1 wt.% PMMA microcapsules at 1000 rpm slightly increased in comparison to the pure epoxy matrix. Nevertheless, the modulus of the specimens in other circumstances decreased (e.g., ~12% reduction in elastic modulus of 2.5 wt.% PMMA microcapsules at 600 rpm). This behavior can be attributed to the incorporation of thermoplastic PMMA shell into the thermoset epoxy matrix that lessens the modules of the matrix. Moreover, another issue that may cause a position slip for the microcapsule surface within the matrix leading to a decrease in the modules of the polymer composite is the weak interfacial adhesion that exists between healing agent capsules and matrix. The morphological properties of the capsule shells have direct effects on interfacial adhesion between the epoxy matrix and the microcapsule wall. The reduction in elastic modulus was also reported for other encapsulation-based healing systems (Yuan *et al*. 2008, Ahangaran *et al*. 2019).

4. Conclusions

Dual-component microcapsules, including low viscosity epoxy and its related hardener were synthesized by the internal phase separation method. The processes were accomplished at two different agitation speeds of 600 and 1000 rpm. The yield of microencapsulated healing agents was obtained in the range of 72-78% and 67-70% for epoxy and hardener microcapsules, respectively. Furthermore, the yield of healing agent capsules increased as the mechanical mixing rate decreased. The chemical structure of microcapsules was characterized by FTIR spectroscopy and the results confirmed successful microencapsulation. Scanning electron microscopic images proved the spherical morphology with a smooth surface of microcapsules. Based on static light scattering results, the D_{50}, D_{90} and average particle size values were the lowest for hardener/PMMA microcapsules at 1000 rpm. Moreover, the mean size of the epoxy/PMMA microcapsules was 7.49 and 5.11 μm for 600 and 1000 rpm, respectively. It can be deduced that emulsion made with a higher mixing rate leads to an increase in microcapsule size. Therefore, an analogy relationship was proposed to predict capsule size at different rotational speeds, which was in good agreement with the experimental values. EPL-1012 epoxy resin was reinforced with homogeneous dispersion and the constant weight ratio of 1:1 of PMMA/epoxy and PMMA/hardener microcapsules. The tensile tests were performed on the specimens filled with microcapsules via the incorporation of 1 and 2.5 wt.% PMMA capsules. The results indicated that the tensile strength of the self-healing composite initially increased for 1 wt.% PMMA capsules at 1000 rpm and then 5%, 10%, and 13% reduction were observed for 2.5 wt.% at 1000 rpm, 1 and 2.5 wt.% at 600 rpm, respectively. In fact, the TS and Young's modulus decreased with the rise in the concentration and mean particle size of PMMA microcapsules.

References

Ahangaran, F., Navarchian, A.H., Mehran, H. and Esmailpour, K. (2016), "Effect of mixing mode and emulsifying agents on micro/nanoencapsulation of low viscosity self-healing agents in polymethyl methacrylate shell", *Smart Mater. Struct*., **25**(9), 095035. https://doi.org/10.1088/0964-1726/25/9/095035

Ahangaran, F., Hayaty, M., Navarchian, A.H. and Picchioni, F. (2017a), "Micromechanical assessment of PMMA microcapsules containing epoxy and mercaptan as self-healing agents", *Polym. Test*., **64**, 330-336. https://doi.org/10.1016/j.polymertesting.2017.10.014

Ahangaran, F., Hayaty, M. and Navarchian, A.H. (2017b), "Morphological study of polymethyl methacrylate microcapsules filled with self-healing agents", *Appl. Surf. Sci*., **399**, 721-731. http://dx.doi.org/10.1016/j.apsusc.2016.12.116

Ahangaran, F., Hayaty, M., Navarchian, A.H., Pei, Y. and Picchioni, F. (2019), "Development of self-healing epoxy composites via incorporation of microencapsulated epoxy and mercaptan in poly(methyl methacrylate) shell", *Polym. Test*., **73**, 395-403. https://doi.org/10.1016/j.polymertesting.2018.11.041

Andersson, H.M., Keller, M.W., Moore, J.S., Sottos N.R. and White, S. (2007), "Self Healing Polymers and Composites", *Self Healing Mater*., **100**, 19-44. https://doi.org/10.1007/978-1-4020-6250-6_2

ASTM International (2014), Standard Test Method for Tensile Properties of Plastics, ASTM D638-14, West Conshohocken, PA, USA.

Bekas, D.G., Tsirka, K., Baltzis, D. and Paipetis, A.S. (2016), "Self-healing materials: A review of advances in materials, evaluation, characterization and monitoring techniques", *Compos. Part B: Eng*., **87**, 92-119. https://doi.org/10.1016/j.compositesb.2015.09.057

Blaiszik, B.J., Kramer, S.L.B., Olugebefola, S.C., Moore, J.S., Sottos, N.R. and White, S.R. (2010), "Self-Healing Polymers and Composites", *Annual Rev. Mater. Res*., **40**(1), 179-211. https://doi.org/10.1146/annurev-matsci-070909-104532

Bolimowski, P.A., Wass, D.F. and Bond, I.P. (2016), "Assessment of microcapsule—catalyst particles healing system in high performance fibre reinforced polymer composite", *Smart Mater. Struct.*, *Int. J.*, **25**(8), 084009. http://dx.doi.org/10.1088/0964-1726/25/8/084009

Drenchev, L. and Sobczak, J.J. (2014), *Self-healing Materials as Biomimetic Smart Structures*, Foundry Research Institute, Krakow, Poland.

Duan, G., Zhang, C., Li, A., Yang, X., Lu, L. and Wang, X. (2008), "Preparation and Characterization of Mesoporous Zirconia Made by Using a Poly (methyl methacrylate) Template", *Nanosc. Res. Lett.*, **3**(3), 118. https://doi.org/10.1007/s11671-008-9123-7

He, Z., Jiang, S., An, N., Li, X., Li, Q., Wang, J., Zhao, Y. and Kang, M. (2019), "Self-healing isocyanate microcapsules for efficient restoration of fracture damage of polyurethane and epoxy resins", *J. Mater. Sci.*, **54**(11), 8262-8275. https://doi.org/10.1007/s10853-018-03236-3

Hillewaere, X.K.D. and Du Prez, F.E. (2015), "Fifteen chemistries for autonomous external self-healing polymers and composites", *Progress Polym. Sci.*, **49-50**, 121-153. http://dx.doi.org/10.1016/j.progpolymsci.2015.04.004

Hu, H., Zhang, L., Yu, R., Yuan, L., Yang, Y., He, X., Wang, J. and Li, Z. (2020), "Microencapsulation of ethylenediamine and its application in binary self-healing system using dual-microcapsule", *Mater. Des.*, **189**, 108535. https://doi.org/10.1016/j.matdes.2020.108535

Kim, S.Y., Sottos, N.R. and White, S.R. (2019), "Self-healing of fatigue damage in cross-ply glass/epoxy laminates", *Compos. Sci. Technol.*, **175**, 122-127. https://doi.org/10.1016/j.compscitech.2019.03.016

Kosarli, M., Bekas, D.G., Tsirka, K., Baltzis, D., Vaimakis-Tsogkas, D.T., Orfanidis, S., Papavassiliou, G. and Paipetis, A.S. (2019), "Microcapsule-based self-healing materials: Healing efficiency and toughness reduction vs. capsule size", *Compos. Part B: Eng.*, **171**, 78-86. https://doi.org/10.1016/j.compositesb.2019.04.030

Kousourakis, A. and Mouritz, A.P. (2010), "The effect of self-healing hollow fibres on the mechanical properties of polymer composites", *Smart Mater. Struct.*, **19**(8), 085021. https:// dx.doi.org/10.1088/0964-1726/19/8/085021

Lee, J., Zhang, M., Bhattacharyya, D., Yuan, Y.C., Jayaraman, K. and Mai, Y.W. (2012), "Micromechanical behavior of self-healing epoxy and hardener-loaded microcapsules by nanoindentation", *Mater. Lett.*, **76**, 62-65. https://doi.org/10.1016/j.matlet.2012.02.052

Li, H., Wang, R., Hu, H. and Liu, W. (2008), "Surface modification of self-healing poly(urea-formaldehyde) microcapsules using silane-coupling agent", *Appl. Surf. Sci.*, **255**(5), 1894-1900. https://doi.org/10.1016/j.apsusc.2008.06.170

Li, Q., Mishra, A.K., Kim, N.H., Kuila, T., Lau, K.T. and Lee, J.H. (2013a), "Effects of processing conditions of poly(methylmethacrylate) encapsulated liquid curing agent on the properties of self-healing composites", *Compos. Part B: Engineering*, **49**, 6-15. https://doi.org/10.1016/j.compositesb.2013.01.011

Li, Q., Siddaramaiah, Kim, N.H., Hui, D. and Lee, J.H. (2013b), "Effects of dual component microcapsules of resin and curing agent on the self-healing efficiency of epoxy", *Compos. Part B: Eng.*, **55**, 79-85. https://doi.org/10.1016/j.compositesb.2013.06.006

Luterbacher, R., Trask, R.S. and Bond, I.P. (2016), "Static and fatigue tensile properties of cross-ply laminates containing vascules for self-healing applications", *Smart Mater. Struct.*, **25**(1), 015003. http://dx.doi.org/10.1088/0964-1726/25/1/015003

Navarchian, A.H., Najafipoor, N. and Ahangaran, F. (2019), "Surface-modified poly(methyl methacrylate) microcapsules containing linseed oil for application in self-healing epoxy-based coatings", *Progress Organ. Coat.*, **132**, 288-297. https://doi.org/10.1016/j.porgcoat.2019.03.029

Omosola, F., Kevin, R. and Biswajit, B. (2014), "Glass fibre polyester composite with in vivo vascular channel for use in self-healing", *Smart Mater. Struct.*, **23**(9), 095017. http://dx.doi.org/10.1088/0964-1726/23/9/095017

Omosola, F., Kevin, R. and Biswajit, B. (2015), "Application of self-healing technique to fibre reinforced polymer wind turbine blade", *Smart Struct. Syst.*, *Int. J.*, **16**(4), 593-606. http://dx.doi.org/10.12989/sss.2015.16.4.593

Schramm, G. (1994), *A practical approach to rheology and rheometry*, Gebrueder Haake, Karlsruhe, Germany.

Sharma, A., Pandey, A., Shukla, D.K. and Pandey, K.N. (2018), "Effect of Self-Healing Dicyclopentadiene Microcapsules on Fracture Toughness of Epoxy", *Materials Today: Proceedings*, **5**(10), 21256-21262. https://doi.org/10.1016/j.matpr.2018.06.526

Souzandeh, H. and Netravali, A.N. (2019) "Self-healing of 'green' thermoset zein resins with irregular shaped waxy maize starch-based/poly(D,L-lactic-co-glycolic acid) microcapsules", *Compos. Sci. Technol.*, **183**, 107831. https://doi.org/10.1016/j.compscitech.2019.107831

Sun, T., Shen, X., Peng, Ch., Fan, H., Liu, M. and Wu, Zh. (2019), "A novel strategy for the synthesis of self-healing capsule and its application", *Compos. Sci. Technol.*, **171**, 13-20. https://doi.org/10.1016/j.compscitech.2018.12.006

Sun, Y., Wang, S., Dong, X., Liang, Y., Lu, W., He, Z. and Qi, G. (2020), "Optimized synthesis of isocyanate microcapsules for self-healing application in epoxy composites", *High Perform. Polym.*, 0954008319897745. https://doi.org/10.1177/0954008319897745

Suryanarayana, C., Rao, K.C. and Kumar, D. (2008), "Preparation and characterization of microcapsules containing linseed oil and its use in self-healing coatings", *Progress Organ. Coat.*, **63**(1), 72-78. http://dx.doi.org/10.1016/j.porgcoat.2008.04.008

Taheri, M.N., Sabet, S.A. and Kolahchi, R. (2020), "Experimental investigation of self-healing concrete after crack using nano-capsules including polymeric shell and nanoparticles core", *Smart Struct. Syst.*, *Int. J.*, **25**(3), 337-343. http://dx.doi.org/10.12989/sss.2020.25.3.337

Theophile, T. (2012), *Infrared spectroscopy: materials science, Engineering and Technology*, IntechOpen, Shanghai, China.

Tong, X.M., Zhang, T., Yang, M.Z. and Zhang, Q. (2010), "Preparation and characterization of novel melamine modified poly(urea–formaldehyde) self-repairing microcapsules", *Colloids Surf. A: Physicochem. Eng. Aspects*, **371**(1-3), 91-97. https://doi.org/10.1016/j.colsurfa.2010.09.009

Trask, R.S. and Bond, I.P. (2006), "Biomimetic self-healing of advanced composite structures using hollow glass fibres", *Smart Mater. Struct.*, **15**(3), 704-710. http://dx.doi.org/10.1088/0964-1726/15/3/005

Ullah, H., Azizli, K.A.M., Man, Z.B., Ismail, M.B.C. and Khan, M.I. (2016), "The Potential of Microencapsulated Self-healing Materials for Microcracks Recovery in Self-healing Composite Systems: A Review", *Polym. Rev.*, **56**(3), 429-485. https://doi.org/10.1080/15583724.2015.1107098

Urdl, K., Kandelbauer, A., Kern, W., Müller, U., Thebault, M. and Zikulnig-Rusch, E. (2017), "Self-healing of densely crosslinked thermoset polymers—a critical review", *Progress Organic Coat.*, **104**, 232-249. https://doi.org/10.1016/j.porgcoat.2016.11.010

Wang, R., Li, H., Liu, W. and He, X. (2010), "Surface Modification of Poly(urea-formaldehyde) Microcapsules and the Effect on the Epoxy Composites Performance", *J.*

Macromol. Sci., Part A, **47**(10), 991-995. https://doi.org/10.1080/10601325.2010.507982

Wang, Y., Pham, D.T. and Ji, C. (2015), "Self-healing composites: A review", *Cogent Eng.*, **2**, 1075686. https://doi.org/10.1080/23311916.2015.1075686

Yan, X., Chang, Y. and Qian, X. (2019), "Preparation and Self-Repairing Properties of Urea Formaldehyde-Coated Epoxy Resin Microcapsules", *Int. J. Polym. Sci.*, 7215783. https://doi.org/ 10.1155/2019/7215783

Yuan, Y.C., Rong, M.Z., Zhang, M.Q., Chen, J., G. Yang, C. and Li, X.M. (2008), "Self-healing polymeric materials using epoxy/mercaptan as the healant", *Macromolecules*, **41**(14), 5197-520. https://doi.org/10.1021/ma800028d

Yuan, Y.C., Rong, M.Z., Zhang, M.Q., Chen, J. and G. Yang, C. (2009), "Study of factors related to performance improvement of self-healing epoxy based on dual encapsulated healant", *Polymer*, **50**(24), 5771-5781. http://dx.doi.org/10.1016/j.polymer.2009.10.019

Zhai, L., Narkar, A. and Ahn, K. (2020), "Self-healing polymers with nanomaterials and nanostructures", *Nano Today*, **30**, 100826. https://doi.org/10.1016/j.nantod.2019.100826

Zhang, H., Wang, P. and Yang, J. (2014), "Self-healing epoxy via epoxy–amine chemistry in dual hollow glass bubbles", *Compos. Sci. Technol.*, **94**, 23-29. https://doi.org/10.1016/j.compscitech.2014.01.009

Zhu, D.Y., Rong, M.Z. and Zhang, M.Q. (2015), "Self-healing polymeric materials based on microencapsulated healing agents: From design to preparation", *Progress Polym. Sci.*, **49-**50, 175-220. http://dx.doi.org/10.1016/j.progpolymsci.2015.07.002

CC